Vegetation responses to late Quaternary climate change in a biodiversity hotspot, the Three Parallel Rivers region in southwestern China

ZhongJing Cheng[a], ChengYu Weng[a,*], JianQiu Guo[b], Lu Dai[a,c], ZhongZe Zhou[d]

[a] State Key Laboratory of Marine Geology, Tongji University, Shanghai 200092, China
[b] School of Computer Science, Chinese University of Geosciences, Wuhan 430074, China
[c] Faculty of Architectural, Civil Engineering And Environment, Ningbo University, Ningbo 315211, China
[d] School of Resource and Environments, Anhui University, Hefei 230000, China

A R T I C L E   I N F O

A B S T R A C T

The late-Quaternary vegetation history of a biodiversity hotspot—the Three Parallel Rivers region (TPRR)—was palynologically studied based on a series of fluvial terrace sediments along the upper Lancang valley, southwestern China. A parallel study on the modern pollen rains in the region shows that the contemporary distribution of species along elevational gradients are distinguished by characteristic pollen assemblages, providing good analogs for the reconstruction of the vegetation history. By analyzing the sediments and pollen recovered from the terraces, a brief history of the region since the late deglaciation is revealed. During the late deglaciation (11–14 ka), the pollen assemblages were particularly rich in *Abies*, *Picea* and *Betula*, indicating a range expansion of the alpine forest during a relatively cold time interval. Meanwhile, co-occurring pollen of *Castanopsis*, Myrtaceae, Caprifoliaceae, Araliacae, Anarcadiaceae, etc. suggests these tropical/subtropical trees, which are distributed in today's evergreen forests to the south of this region, once extended into these valleys under a wetter climate. However, since the mid-Holocene, the evergreen tropical/subtropical forests have given way to savanna, as revealed from the corresponding pollen assemblages of the second terrace (4–7 ka). The alpine vegetation might have simultaneously contracted to higher elevations under a warmer climate, and subsequently retreated to its present distribution in response to the late-Holocene cooling. Our first glimpse into the Quaternary vegetation history of the TPRR provides new insights into the mountainous biotic response to climatic forcing, and therefore has important implications for diversification in these steep gorges.

1. Introduction

Located at the southeast edge of Tibetan Plateau, the Three Parallel Rivers region (TPRR) features some of the deepest and most spectacular gorges on Earth (Fig. 1A). For a long time, this mountainous region has earned worldwide attention for its extraordinary geomorphology and biodiversity (e.g., Schweinfurth, 1975; Wu, 1988; Myers et al., 2000; UNSCO, 2003). It is commonly believed that the high species richness there was strongly influenced by the Quaternary climatic fluctuations. For instance, the vertical migration of plant species in response to the glacial-interglacial temperature changes might have promoted the gene flows and eventually more chances for speciation (Li, 1995; Nie et al., 2005); and the mountains and gorges might have served as glacial refugia of montane species (Li, 1995; Cun and Wang, 2010). However, there is still a dearth of direct and clear fossil evidence for such processes because of poor preservation of the Quaternary sediments in these steep gorges.

Recent palynological studies about the Tibetan Plateau also emphasized the effects of monsoon variability on the assembly of vegetation, particularly after the last glacial, a period which could be revealed by most lacustrine and peat deposits. The spread of arid vegetation at the expense of alpine meadows on the plateau during the late Holocene was widely attributed to the weakening of the Indian summer monsoon (e.g. Kramer et al., 2010; Li et al., 2011; Wischnewski et al., 2011; Herzschuh et al., 2014). Similarly, the forest decline on the periphery of the Tibetan Plateau was interpreted to reflect a significant decline in late-Holocene humidity (Shen et al., 2005; Zhao et al., 2011; Xiao et al., 2014).

After climbing up over a series of high mountains on the southwest, the air masses from the Indian Ocean have lost most of their moisture before reaching the TPRR (Fig. 1C), leading to a quite unique arid climate in the so-called dry-hot valleys (Ma and Jack, 2001). Thus, these deep valleys at the fringe of the Indian summer monsoon region are very sensitive to the monsoon variations. A long-term history of the

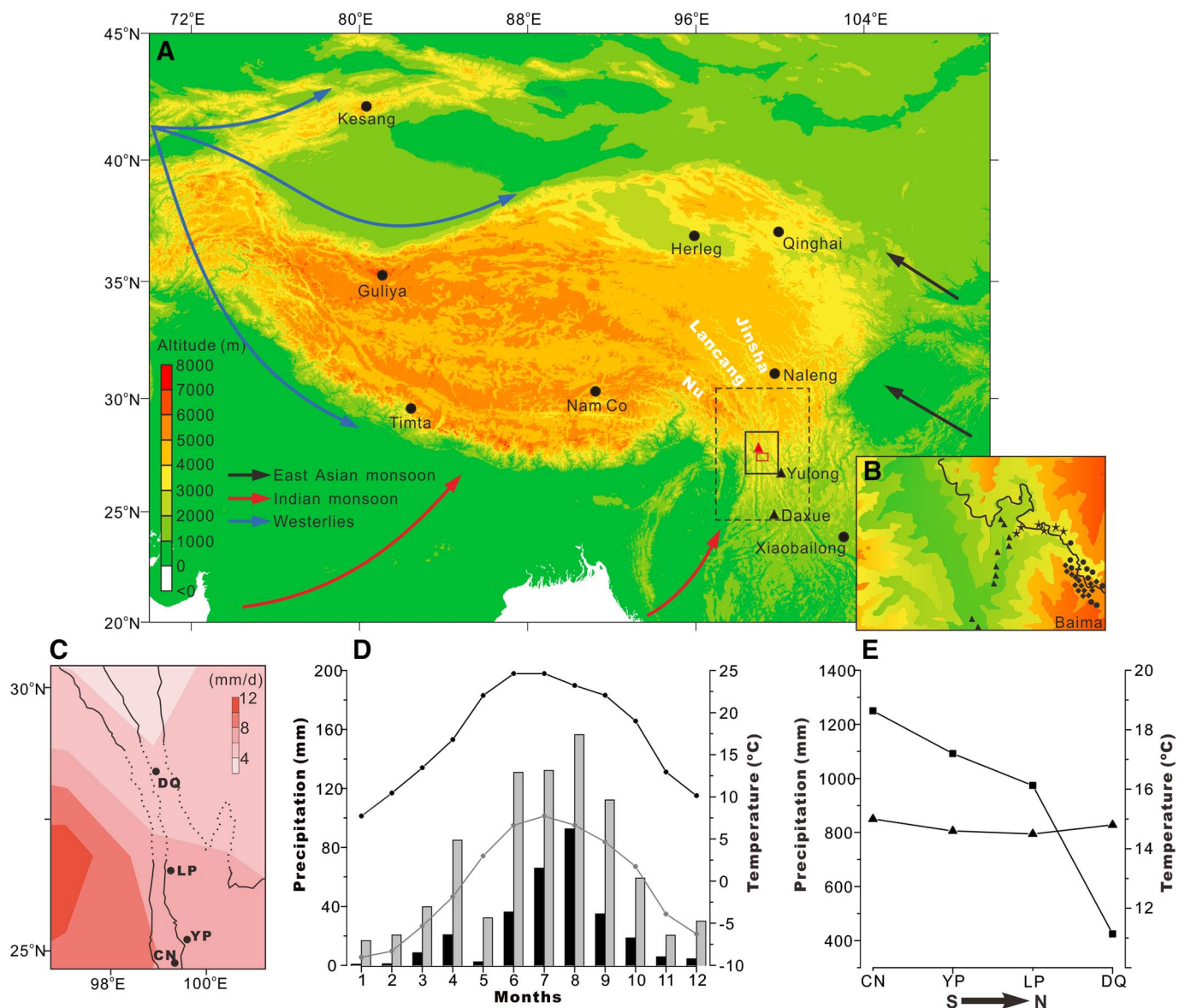**Fig. 1.** (A) Locations of our study sites (red triangle: the fluvial terraces; red box: modern surface sample area, see B for more details) and general directions of wind systems on topographic map of the Tibetan Plateau. The Three Parallel Rivers region (solid box) is the central and steepest part of the Hengduan Mountains Area (dashed box). Some pertinent paleoclimate records (black dots) and modern pollen rain records (black triangles) discussed in the text are also shown. (B) Moss-polster sampling sites on an elevation transect, west flank of the Baima Snow Mountain. Diamonds: Alpine shrub samples. Circles: *Abies* forest samples. Stars: mixed forest samples. Triangles: savanna samples. Crosses: Alpine meadow samples. Black line depicts the Yunnan-Tibetan road. (C) Summer (JJA) precipitation rates (from GPCP data) in the Hengduan Mountains Area. Dotted sections represent the dry-hot valleys. Meteorological stations along the Lancang River: CN, Changning, YP, Yongping, LP, Lanping, DQ, Deqin. (D) Monthly mean precipitation (bars) and monthly mean air temperature (curves) from DQ meteorological station at different elevations: gray, 4500 m, black: 2000 m. (E) Mean annual temperature (squares) and mean annual precipitation (triangles) at ~2000 m elevation of different meteorological stations (shown in C) along the Lancang River. (For interpretation of the references to color in this figure legend, the reader is referred to the web version of this article.)

vegetation changes in these valleys may provide good insights into the influence of monsoon variability on ecological processes in this biodiversity hotspot.

To investigate the late Quaternary vegetation history in the TPRR, here we report a series of fluvial terraces along one of the three great rivers (Lancang River), and present the first palynological record in the deep gorges. To understand the fossil pollen data more precisely, an investigation on the modern pollen rain was conducted along an elevational transect to have a detailed correlation between the modern pollen assemblages and the vegetation along altitudinal gradients in this special region.

2. Regional setting and study sites

The TPRR encompasses approximately 95,000 ha in Yunnan Province, southwestern China. The upper sections of three major Asian rivers, Jinsha (Yangtze), Lancang (Mekong) and Nu (Salween), run parallel from north to south through the gorges which, in places, are > 3000 m deep and are bordered by glaciated peaks > 6000 m high (Fig. 1A).

2.1. Climate

> 80% of the precipitation in the TPRR occurs in summer, from the humid air masses brought in by the Indian summer monsoon. The winter is cold and dry. The precipitation increases with elevation,
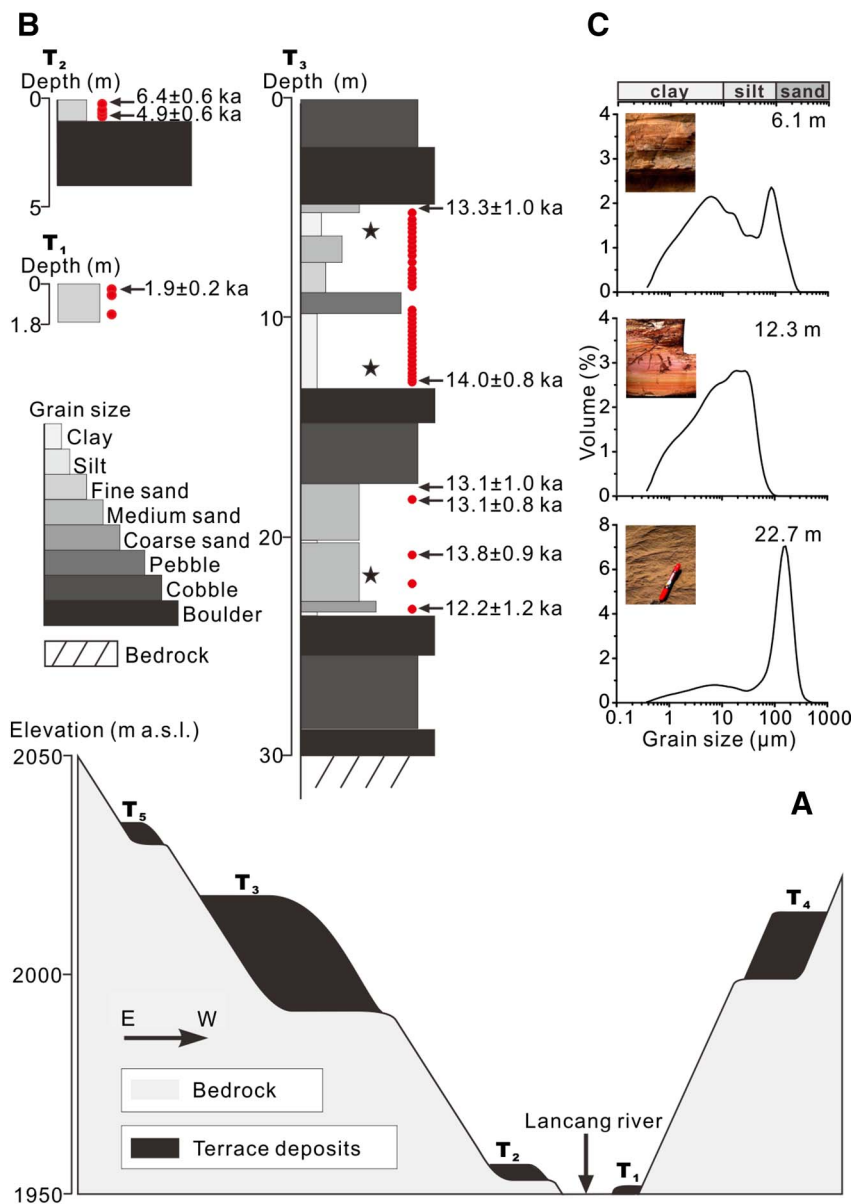
Fig. 2. Lithology of the fluvial terraces in upper Lancang valley. (A) Structures of the terrace profiles in upper Lancang valley. (B) Lithostratigraphy of the first (T_1), second (T_2) and third terrace (T_3). Arrows depict the depths of OSL samples. Depths of samples in which pollen counts > 200 are shown by red dots. Stars show the depths of grain size samples shown in C. (C) Typical grain size distribution curves and sedimentary structures of T_3. (For interpretation of the references to color in this figure legend, the reader is referred to the web version of this article.)

especially above 3000 m; the annual precipitation is 300–400 mm at the elevation of 2000 m, but about 1000 mm at 4500 m. The temperature in the valleys varies with a lapse rate of ∼7 °C per 1000 m elevation, and the mean annual temperature is at around 15 °C at 2000 m. (Zhang et al., 1997; Li and Zhang, 2010) (Fig. 1D).

As the moisture-bearing air masses brought in by the Indian summer monsoon are mostly blocked by the southern slopes, there is a sharp precipitation gradient from lower reaches to the TPRR (Fig. 1C). But due to the strong foehn effect (Li and Zhang, 2010), the temperature change is negligible on the same route (Fig. 1E). This pattern leads to a dry-hot climate in the interior deep valleys. The monsoonal climate regime thus plays a prominent role in the vegetation difference from lower to upper reaches of these large rivers.

2.2. Vegetation

The most prominent feature of the vegetation in the TPRR is the niche differentiation of plant species along the altitudinal gradient. Moisture from the Indian Ocean seldom reaches the valley bottoms, and a special type of arid savanna vegetation developed at the low elevations of the dry-hot valleys. According to our field work on the west

flank of the Baima Snow Mountain (28°23′01″ N, 99°00′21″ E, peak: 5430 m) and the published references (Li and Li, 1993; Zhang et al., 1997; Guo, 2004; Li and Zhang, 2010), the vegetation can be generally divided into 5 broad types:

1) *Savanna*: between the elevations of 1900 m and 3000 m, characterized by the widespread herbs like *Artemisia* (Asteraceae), Amaranthaceae, *Heteropogon contortus* (Poaceae), *Themeda triandra*, *T. gigantean* (Poaceae), *Eulaliopsis binata* (Poaceae). Some trees such as *Juglans sigillata* (Juglandaceae), *Quercus franchetii* (Fagaceae), *Platycladus orientalis* (Cupressaceae), *Bombax malabarica* (Bombacaceae), *Pistacia weinmannifolia* (Anarcadiaceae), *Sargeretia pycnophylla* (Rhamnaceae) and shrubs such as *Acacia farnesiana* (Leguminosae), *Sophora vicifolia* (Leguminosae), *Bauhinia variegate* (Leguminosae), *Vitex negundo* (Verbenaceae), *Wikstroemia gemmata* (Thymelaeaceae) could also be seen scattered. Succulent thorny shrubs such as *Opuntia monacantha* (Cactaceae) and *Euphorbia antiquorum* (Euphorbiaceae) occur below 2300 m elevation.

2) *Coniferous and broad-leaved mixed forests*: between 3000 m and 3800 m. *Pinus yunnanensis* is the most widely distributed coniferous species, which is mixed with trees of *Tsuga*, *Cupersus duclouxiana*

and *Larix* sp. The common broad-leaved trees include *Quercus pannosa*, *Q. senescens*, *Schima argentea* (Theaceae), *Alnus nepalensis*, Aceraceae, *Fraxinus* (Oleaceae), *Ligustrum lucidum* (Oleaceae), etc.

3) *The Abies forests*: between 3800 m and 4100 m, dominated by *Abies* trees, but accompanied by the trees of *Picea*, *Tsuga*, *Quercus aquifolioides*, *Sorbus* (Rosaceae), *Betula utilis*, *B. platyphylle*, *Populus davidiana* and *Salix*.

4) *Alpine shrubs*: between 4000 m and 4350 m, mainly formed by the *Rhododendron* (Ericaceae) shrubs, with some scattered stunted trees of *Abies*, *Quercus* and *Betula*.

5) *Alpine meadows*: between 4350 m and 4500 m, basically covered with extensive herbs, but stunted *Rhododendron* and *Sabina squamata* (Cupressaceae) shrubs are occasionally found. The herbs are mainly composed of *Kobresia* (Cyperaceae), *Carex* (Cyperaceae), *Festuca rubra* (Poaceae), *Anaphalis flavescens* (Asteraceae), *Polygonum marophyllum*, *P. viviparum* (Polygonaceae), *Leontopodium longifolium* (Asteraceae), *Spenceria ramalana* (Rosaceae), *Ranunculus pulchellus* (Ranunculaceae) etc.

2.3. Sampling sites

Five fluvial terraces were found in the study area, the upper Lancang valley, between 28.608°N, 98.757°E and 28.275°N, 98.842°E, Deqin County. The elevations of the terraces range from 1950 m to 2100 m (Fig. 2A), at which the landscapes are occupied by savanna today. The modern pollen rain study was conducted on the west flank of Baima Snow Mountain from 28.290°N, 98.871°E to 28.338°N, 99.005°E, adjacent to the Yunnan-Tibetan Road (Fig. 1B). The modern samples were collected from 1960 m to 4405 m elevation, covering all the five vertically distributed vegetation types.

3. Materials and methods

3.1. Modern pollen samples

A total of 39 moss polster samples were collected at intervals of 50–200 m elevations (Fig. 1B). Pollen and spores were extracted by physical-chemical treatments including 30% HCl (24 h), 10% KOH (10 min at 90 °C), and sieving at 200 μm and 7 μm in turn. Pollen identifications were based on published atlases and keys (Wang et al., 1991; Fujiki et al., 2005) and modern pollen references collected in this region by Zhou. At least 300 terrestrial pollen grains were counted for each sample. Percentages of pollen were counted on pollen sum and percentages of fern spores were calculated based on the total sum of pollen and spores (Fig. 3).

Principle Components Analysis (PCA) was performed using CANOCO program after excluding the minor taxa whose maximum values are below 5%. Pollen percentages were square-root-transformed in PCA in order to downweight the abundant types.

3.2. Sediment samples from the terraces

The pollen samples were collected in each terrace profile. For each sample, 20 g clay or 40 g sand were taken at an interval of 20 cm. While in gravel layers, 80 g interstitial materials were taken. Pollen samples were processed following the standard procedure, including 30% HCl, 55% HF and fine sieving to remove particles < 7 μm. For most samples, > 300 pollen grains per sample were counted, except for those in which pollen concentrations were too low. Pollen percentages were based on the pollen sum and spore percentages were calculated using the total sum of pollen and spores.

To measure the grain sizes, a series of samples of 3 g sediments were collected at 10 cm intervals from sand and clay layers of the third terrace, and were pretreated with chemicals including H_2O_2, HAc and SHMP, and then measured using a Beckman Coulter LS230 Laser Particle Analyzer.

Six samples from the third terrace, two samples from the second terrace and one sample from the first terrace were selected for optical stimulated luminescence (OSL) dating in the OSL lab of Peking University.

4. Results

4.1. Modern pollen assemblages along the elevational gradient

The pollen assemblages vary with the elevations. *Pinus* pollen is basically abundant in all samples, and the pollen of *Tsuga*, Moraceae, *Alnus*, Asteraceae, Cupressaceae, *Populus*, Myrsinaceae and Araliaceae each shows little variation along the whole transect. But most taxa show quite clear elevational patterns and are well correlated with the vegetation (Fig. 3).

1) *Dry-hot valley savanna* (1900–3000 m): the pollen percentage of *Artemisia* is generally high but highly variable (1%–53%, average 20%). *Juglans* (2%–13%), Amaranthaceae (0.5%–7%) and Poaceae (< 7%) are moderately abundant and persistently characterize these elevations. Euphorbiaceae (< 5%), Rubiaceae (< 6%), Thymelaeaceae (< 3.5%), Labiatae (< 6%), Zygophyllaceae (< 0.5%) are common here but absent at higher elevations. *Abies* (< 6%), *Picea* (< 2%), *Quercus* (2%–10%) are rare.

2) *Coniferous and broad-leaved mixed forests* (3000–3800 m): peak values of *Artemisia*, *Quercus* and *Pinus* alternatively occur, but the percentages are also most variable in the whole transect. 3550 m is a notable boundary between low (e.g. *Artemisia*) and high (e.g. *Abies* and Ericaceae) elevation components.

3) *Abies forests and alpine shrubs* (3800–4350 m): the two zones are distinct along the whole transect but not quite distinguishable from each other. These elevations are characterized by abundant *Abies* (10%–30%), *Betula* (3%–15%) and *Quercus* (10%–30%). *Picea*, Rananculaceae, *Salix* and Ericaceae are modest but important. Two peak values of Caryophyllaceae exceed 30%. Rosaceae is moderately abundant in *Abies* forest.

4) *Alpine meadows* (4350–4450 m): tree pollen diversity decreases obviously in this zone except for the most common types like *Pinus* (7%–29%) and *Quercus* (7%–23%). Ericaceae is still abundant (8%–20%). Herbaceous pollen of Polygonaceae (7%–29%), Cyperaceae (2%–9.5%), Geraniaceae (< 0.5%), Gentianaceae (< 1.5%), Primulaceae (< 0.5%), *Typha* (< 1%), Crassulaceae (< 1.5%) and Onagraceae (< 1%) etc. dominates the pollen rain. *Abies* (< 6.5%) and *Artemisia* (< 4%) are rare.

The statistical analysis (PCA) results (Fig. 4) also support a clear differentiation between the low and high elevations. The first two axes of PCA explain 48% of the total variance (eigenvalue 0.299 for Axis 1, eigenvalue 0.181 for Axis 2). In general, the high elevation components have the most positive scores on Axis 1, such as Ericaceae, Polyganaceae, *Picea*, *Abies* and *Quercus*, while the low elevation components, such as *Artemisia*, Amaranthaceae, Euphorbiaceae, *Juglans* and Thymelaeceae, have highly negative scores. Correspondingly, the valley savanna samples are located at the left part of the plot while the alpine samples at the right part and alpine meadow samples to the rightmost. A secondary analysis including elevation as environment variable (RDA) reveals the first axis correlates closely with a gradient of increasing elevation (79.6%). This pattern is confirmed by linear regression of the elevation and the PCA Axis 1 scores ($R^2 = 0.6564$). Axis 2 is mainly controlled by the fluctuations of several dominant taxa such as *Pinus*, *Artemisia* and *Quercus* which contribute the highest scores.

4.2. Lithology of the terraces

The deposits of the five terraces are not equal in depth. The outcrop of the first terrace is 1.8 m thick, with the bedrock still submerged
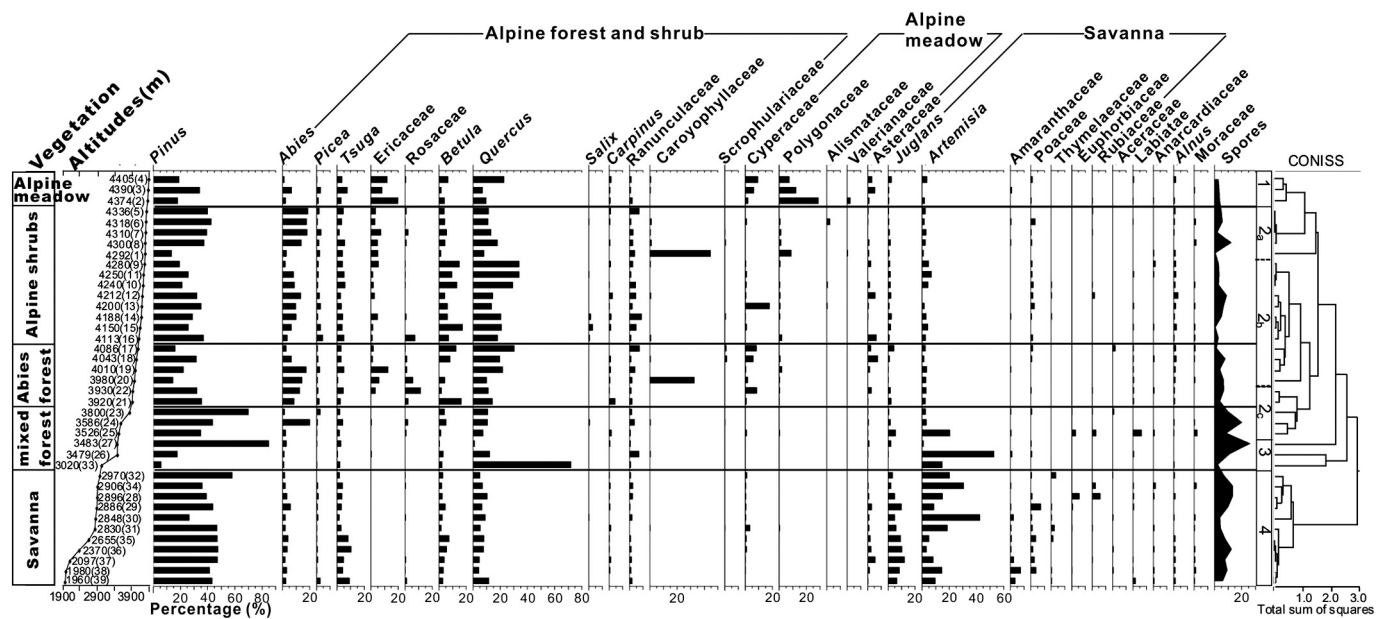
Fig. 3. Pollen percentage diagram and CONISS-based pollen zones of modern surface pollen samples. Sample IDs are listed behind the elevation.

today. The outcrop of the second terrace is 4.8 m thick, with the top and bottom parts covered by modern slope deposits. The 30 m thick third terrace profile is best exposed, stretching about 100 m along the meandering riverbank. The strongly weathered fourth and fifth terrace profiles are 4.5 m and 3 m thick, respectively.

As pollen grains were not found in the fourth and the fifth terrace,

most probably due to severe weathering, the details are thus beyond the scope of this article.

The third terrace profile is best developed and the thickest among the five terraces. It includes three normal graded bed sequences, each of which consists of a gravel bed, a sand bed and a clay bed from bottom to top (Fig. 2B). The base sequence is dominated by gravels and
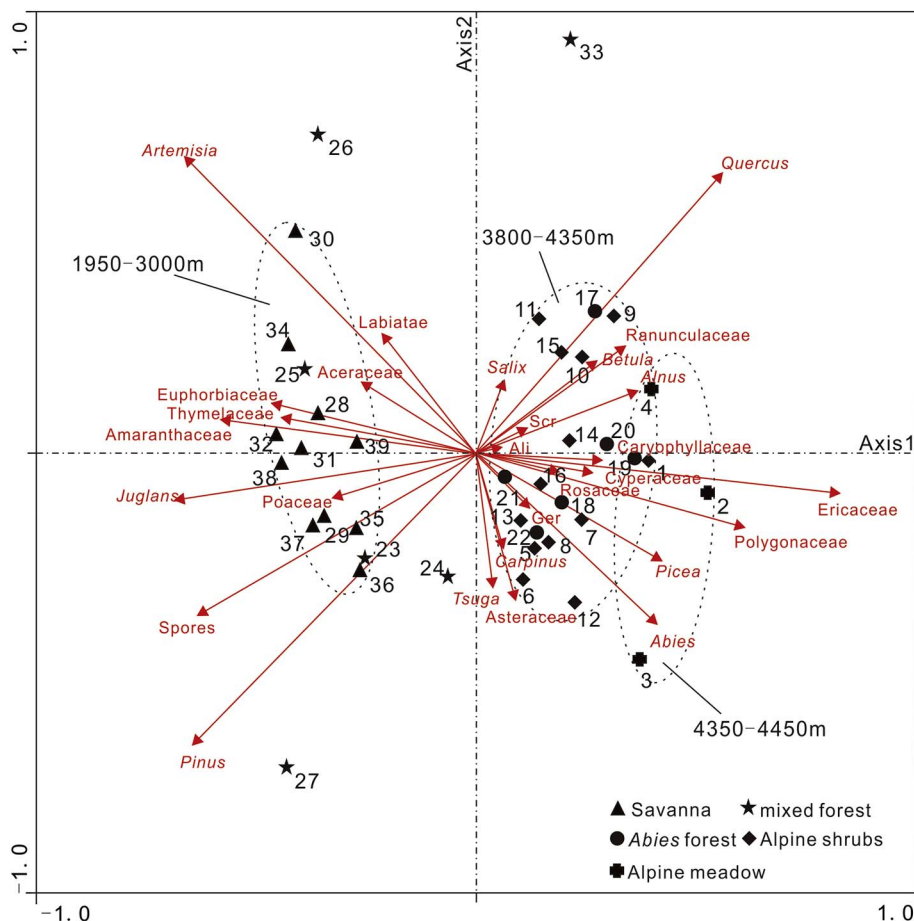

Fig. 4. Plot of PCA results of modern surface samples on the first two axes. The scaling of ordination scores is focused on inter-species correlations. The elliptical circles delimit samples from different elevation zones.

Table 1
OSL dating samples and results.

Profile	Depth (m)	Lab ID	Grain size (μm)	U (ppm)	Th (ppm)	K (%)	Dose rate (Gy/ka)	De (Gy)	Age (ka)
T$_1$	0.1	L1734	90–125	1.85 ± 0.07	7.45 ± 0.25	1.44 ± 0.05	2.1 ± 0.2	4.06 ± 0.11	1.9 ± 0.2
T$_2$	1.7	L1735	90–125	2.36 ± 0.08	9.61 ± 0.29	1.69 ± 0.05	2.5 ± 0.1	12.31 ± 1.44	4.9 ± 0.6
T$_2$	0.1	L1736	90–125	2.25 ± 0.09	9.28 ± 0.28	1.66 ± 0.05	2.5 ± 0.1	15.65 ± 1.18	6.4 ± 0.6
T$_3$	24.3	L1737	90–125	3.15 ± 0.11	13.5 ± 0.38	2.62 ± 0.07	3.6 ± 0.2	44.46 ± 3.84	12.2 ± 1.2
T$_3$	22.2	L1738	90–125	1.94 ± 0.08	7.82 ± 0.25	1.57 ± 0.05	2.2 ± 0.1	30.86 ± 1.47	13.8 ± 0.9
T$_3$	19	L1739	90–125	1.78 ± 0.07	7.22 ± 0.25	1.51 ± 0.05	2.1 ± 0.1	27.98 ± 0.93	13.1 ± 0.8
T$_3$	18.5	L1740	90–125	2.18 ± 0.08	8.20 ± 0.26	1.52 ± 0.05	2.3 ± 0.1	29.83 ± 1.64	13.1 ± 1.0
T$_3$	14.2	L1741	63–90	2.60 ± 0.09	10.8 ± 0.32	1.66 ± 0.05	2.6 ± 0.1	36.89 ± 1.20	14.0 ± 0.8
T$_3$	5.7	L1743	90–125	2.47 ± 0.09	9.77 ± 0.29	1.53 ± 0.05	2.4 ± 0.1	32.31 ± 1.99	13.3 ± 1.0

medium sands while the medium and top sequences are dominated by silts and clay. Cross-bedding is common in the gravel beds. Sedimentary structures within the sand beds usually consist of climbing ripples (Fig. 2C, 6.1 m), cross-bedding and parallel bedding, and within the clay beds consist of horizontal bedding (Fig. 2C, 12.3 m), lenticular bedding (Fig. 2C, 22.7 m) and occasionally flame structure. The grain size distribution curves reveal that the sediment particles from the lower part of the profile are well sorted, with the medium sand being the most abundant fraction, but in the upper part of the profile are only moderately or poorly sorted, with few silt or fine sand mixed within the clay beds (Fig. 2C).

The outcrop of the second terrace consists of 3 m gravel bed at the bottom and 1 m silt bed mixed with clay at the top. The outcrop of the first terrace is mainly dominated by medium/fine sands (Fig. 2B). Sedimentary structures within both terraces are climbing ripples and cross-bedding.

4.3. Chronology

The OSL dating (Table 1) constrains the terrace deposits into three time intervals: the third terrace during the late deglaciation (11–14 ka), the second terrace during the mid-Holocene (4–7 ka) and the first terrace during the late Holocene (~2 ka). Although the median ages are not always in stratigraphic order, there is no anomalous age within error. The three time intervals are in agreement with base levels of different terraces, suggesting a persistent down-cutting of the river. Moreover, our results can be compared with a number of fluvial terrace datings around the Tibetan Plateau (Ji et al., 2000; Wang et al., 2009; Dutta et al., 2012) that may imply a common forcing of the regional late-Quaternary terrace formation. A more detailed investigation into the intra-terrace variations is hampered by insufficient organic material to provide radiocarbon (AMS ^{14}C) ages.

4.4. Fossil pollen results

In most cases, pollen grains were not found or too rare for statistical analysis in the coarse/medium sand and gravel layers. Most good pollen data were recovered from the fine-grained sediments (fine sands or clay). A total of 48 valid data sets with enough pollen grains were obtained eventually, with 41 from the third terrace, four from the second terrace and three from the first terrace (Fig. 2). The summary pollen diagram is shown in Fig. 5.

4.4.1. The first terrace (~2 ka)

The three samples from the first terrace show very similar pollen compositions. *Pinus* pollen, averaging 50%, is the most dominant taxon in all three samples. *Abies* and *Picea* pollen composes about 10% of the pollen sum. *Tsuga* and broadleaved tree pollen percentages are low. The most abundant herbaceous component is Cyperaceae with a mean value of 9%; other types are generally under 3%. Fern spores are only about 10%.

4.4.2. The second terrace (4–7 ka)

This profile is distinguished by high percentages of the arid taxa *Artemisia* and Amaranthaceae (up to 63%). Thymelaeaceae (up to 36.5%) is the most important shrub pollen type. *Abies* and *Picea* reach their minimum values in all the three terraces. Anacardiaceae pollen (4%–8%) and fern spores (~30%) are moderately abundant.

4.4.3. The third terrace (11–14 ka)

Abundant *Abies* pollen (mostly between 10%–31%) is quite characteristic. *Picea* pollen is usually ~5%, occasionally exceeds 10%. *Pinus* pollen basically maintains a high level (mean of 26%), though fluctuates widely (between 5%–80%). Pollen of Poaceae and Cyperaceae is also strikingly more abundant than in the later two stages, basically between 10% and 50%, but *Artemisia* and Amaranthaceae pollen is much less than in the second terrace.

Taxodiaceae is common. The broadleaved tree pollen types are very common and diverse, including both the temperate and tropical components such as *Castanopsis*, Myrtaceae, Araliaceae, Rubiaceae, Caprifoliaceae, Proteaceae, Leguminosea, etc. *Betula* (up to 15%) is the most abundant broadleaved tree pollen. Herbaceous pollen is important. Besides Poaceae and Cyperaceae, Polygonaceae, Asteraceae and Ranunculaceae also maintain relatively high values. Caryophyllaceae, *Artemisia*, Amaranthaceae, *Ephedra* are common and Scrophulariceae, Liliaceae, Onagraceae, Berberidaceae, etc. also consistently appear.

Aquatic pollen is rare. A large amount of fern spores (up to 3 times more than pollen) also characterize the third terrace. Besides, it is noteworthy that certain pollen types, such as Anarcadiaceae, Aceraceae, *Castanopsis*, Verbenaceae, Caprifoliaceae, Poaceae, Cyperaceae, and Geraniaceae, would briefly increase to extreme abundances.

5. Discussion

5.1. Modern pollen rain and its indication for vegetation types

5.1.1. Indicative pollen assemblages for vegetation types in the TPRR

Pollen rain of the dry-hot valley savanna is characterized by abundant arid herbaceous pollen, particularly *Artemisia*, Poaceae and Amaranthaceae. It is noteworthy they are also typical pollen types of alpine steppe over the Tibetan Plateau (Yu et al., 2001; Shen et al., 2006; Zhao and Herzschuh, 2009; Wei et al., 2011), the upper stream region of the river. Nonetheless, a variety of co-existed pollen taxa from the associated trees and shrubs like *Quercus*, *Juglans*, Thymelaeaceae, Euphorbiaceae, Rubiaceae, Anacardiaceae, Zygophyllaceae and Leguminosae, may well distinguish this unique ecological unit.

The coniferous and broad-leaved mixed forest is somehow obscured in the pollen spectra. A lack of characteristic pollen assemblages in these samples leads to poor clustering in CONISS analysis and the PCA plot (Figs. 3 & 4). Pollen of the dominant species, *Pinus* spp. and *Quercus* spp. does not seem to clearly reflect the local occurrence of the mixed forests. *Pinus* pollen, given its high productivity and well-known ability
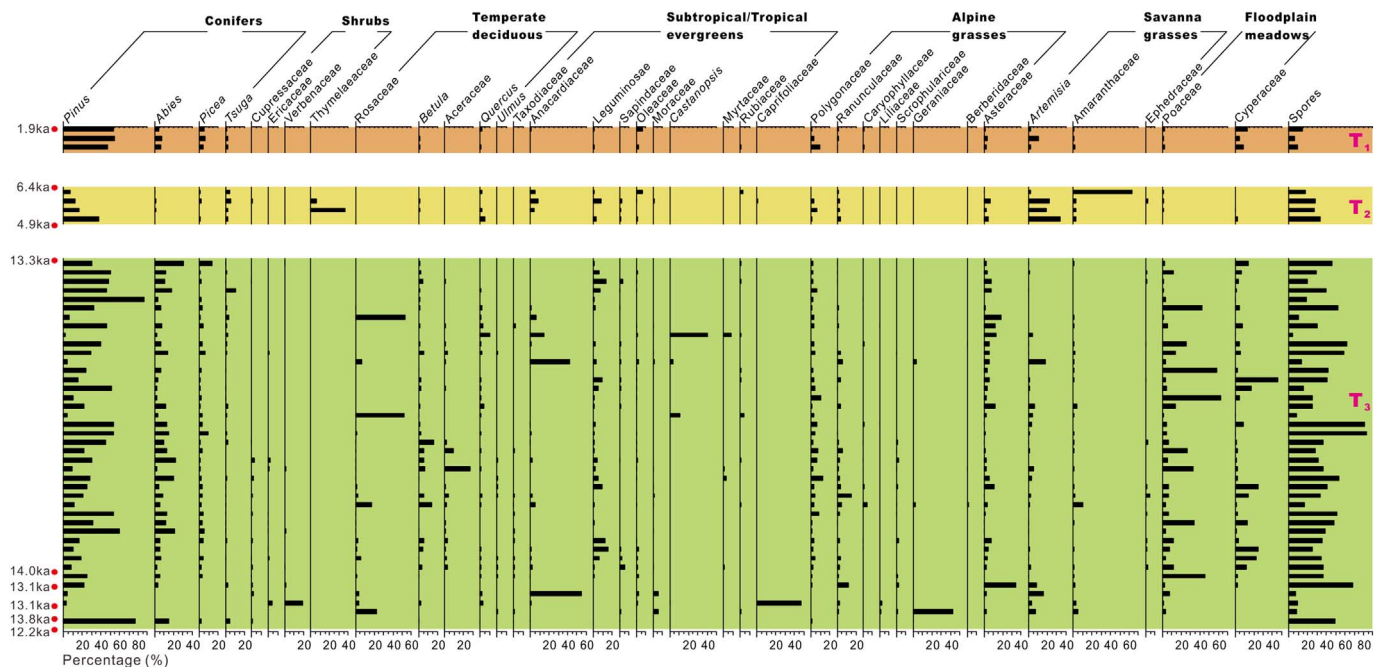
Fig. 5. Pollen percentage diagram from the terrace profiles in upper Lancang valley. The percentages are plotted in stratigraphical order as shown in Fig. 2.

of long-distance dispersal, is not unexpected to dominate nearly the whole transect. Differently, *Quercus* pollen is not so indicative most probably because of a low taxonomical resolution. In the TPRR, *Quercus franchetii* from the savanna adapts to the dry-hot climate at low elevations, *Q. aquifolioides* preferring the alpine environment is common in the *Abies* forests and *Q. pannosa*, *Q. senescens* are distributed in the coniferous and broadleaved mixed forest. However, their pollen is not possible to differentiate (Jarvis et al., 1992). By comparison, *Quercus* pollen is quite characteristic for the mixed forests on the Yulong Mountain (Xiao et al., 2009) where the savanna and alpine *Quercus* forests are rarely developed. Additionally, the local human disturbances are most intense at the elevations for this vegetation type, so the deforestation may also depress the pollen production of this zone and increase the relative abundances of pollen from neighboring zones, such as *Abies* and *Artemisia*.

Abies, *Betula*, *Quercus* and Ericaceae are the most significant pollen types for the alpine forests and alpine shrubs. But the increasing population density of Ericaceae shrubs with elevation is not apparent in terms of pollen percentage. This may be due to the lower pollen productivity of alpine shrubs than alpine trees. Ericaceae pollen is absent below 3500 m elevation because of poor dispersal, making its presence perhaps the most reliable indicator of the alpine environments. Rosaceae pollen is also important as it exhibits a very narrow elevational range. The understory herbs are well distinguished by pollen assemblages including Ranunculaceae, Cyperaceae, Caryophyllaceae, Scrophularieceae, Primulaceae, Geraniaceae, Gentianaceae, etc.

While approaching the mountain ridges, strengthened valley breezes carry a large number of pollen upslope, leading to overwhelming Ericaceae, *Pinus* and *Quercus* pollen in the alpine meadow. Nevertheless, moderately abundant Polygonaceae, Cyperaceae, Ranunculaceae and Asteraceae are viable indicators of this habitat type. More abundant Polygonaceae and less Cyperaceae also differentiate alpine meadow from habitats on the Tibetan Plateau (Yu et al., 2001; Shen et al., 2006; Zhao and Herzschuh, 2009; Wei et al., 2011).

A summary of pollen indicators for different vegetation types can also been found in the PCA plot (Fig. 4). In general, the taxa clustered at the left section represent the savanna vegetation while those at the right section represent the alpine vegetations and the most positive taxa give a differentiation of the alpine meadow.

5.1.2. Comparing modern pollen rain from lower to upper reaches of the three rivers

Few investigations of modern pollen rain have been made in the mountainous southwestern China. Two previous studies were conducted to the south of the TPRR (Fig. 1A): one along an elevational transect from 2200 m to 4100 m on the eastern slope of Yulong Mountain (between 27.010°N, 100.167°E and 27.167°N, 100.251°E), middle Jinsha valley (Xiao et al., 2009); another below 3000 m on the western slope of Daxue Mountain (~24.833°N, 99.733°E), lower Lancang valley (Pan et al., 2009). By comparing these studies, a glimpse of how pollen rain may differ along a precipitation-induced eco-cline could be obtained. Yulong is to the south of our study site Baima, and Daxue is further southern. The temperature is not significantly different among these three sites, below 3000 m elevation in the Daxue transect, the mean annual temperature is about 9.5–17 °C, while in the Yulong transect 10.2–14.8 °C and the Baima transect 8–15 °C. However, the precipitation is apparently different, from south to north, the mean annual precipitation decreases from 1600 to 3500 mm, 800–1100 mm to 400–500 mm. Correspondingly, the vegetation changes from evergreen broadleaved forests, to the coniferous and broadleaved mixed forests, and then to the valley savanna.

The pollen assemblages on Daxue Mountain show a dominance of *Castanopsis* (~30%). Other broadleaved evergreen taxa, like Oleaceae, Hamamelidaceae, Araliaceae, Anacardiaceae, *Quercus*, are moderately abundant (5%–15%), but they together give a major contribution. Both *Pinus* and Poaceae are < 5% (Pan et al., 2009). On the Yulong Mountain, *Pinus* pollen dominates the pollen rain (up to 90%). *Castanopsis* pollen still maintains a relatively high abundance but the proportions are quite variable (0–60%). *Quercus* pollen on average is higher (~30%) than on the Daxue Mountain. Herbaceous pollen is rare but with a consistent occurrence of *Artemisia* (< 3%) (Xiao et al., 2009). On the Baima Mountain, *Castanopsis* pollen further dwindles to sporadic appearance, whereas substantial herbaceous pollen characterizes the assemblages. Amaranthaceae, Thymelaeaceae and *Juglans* are moderately abundant and important, but seldom appear to the south.

5.2. Evolution of the vegetation and environments in the region

5.2.1. Sedimentary facies and pollen provenance of the terrace deposits

The lithology, sedimentary structure and crescent-shaped morphology indicate the terrace sequences correspond to point bar and floodplain deposits of a fluvial system. So before extrapolating the modern relationship between pollen and vegetation to the past, one should note the fluvial pollen could be either airborne (as expressed in moss-polster samples) or waterborne, or most probably be both. A few previous studies suggest that fluvial pollen deposits integrate both the regional vegetation signal over catchment area and local signals from the point bar, floodplain, etc. (Fall, 1987; Xu et al., 1996; Zhu et al., 2002). The local signals are usually strengthened closer to the lower stream as the swamps and marshes increase (Chmura and Liu, 1990; Xu et al., 1996; Chmura et al., 1999; Zhu et al., 2003). Pollen types were found to be well mixed in both lakes and rivers (Hall, 1989; Simirnov et al., 1996; Holmes, 1990, 1994; Brown et al., 2008). However, some pollen types were observed to be relatively enriched in the sediments probably because their blossom times are in phase with floods (Simirnov et al., 1996). Pollen load during flood periods is usually 10 times higher than normal (Peck, 1973; Bonny, 1978; Brown, 1985; Brown et al., 2008); if the plants happen to be in blossom, huge amounts of pollen are directly injected into the river and consequently deposited in the fluvial sediments. Another possibility is that these pollen types tend to be better preserved in coarser sediments. These may partly be the reason why hydrodynamic sorting was recorded in different sedimentary facies (Xu et al., 1996).

Despite the complexity of fluvial pollen provenance, there are some good signs to indicate that our terrace deposits are reliable in unveiling vegetation history of the TPRR. Firstly, the fossil pollen assemblages well match the modern pollen rain of this region, but are distinct from the modern and fossil pollen assemblages of the headwater regions, northern Tibetan Plateau. For instance, the abundant fern spores and diverse tree pollen including subtropical evergreens, temperate deciduous and alpine conifers are unlikely from the Tibetan Plateau, where most landscapes have been occupied by alpine steppes, alpine meadows or deserts since the Last Glacial Maximum (e.g. Wischnewski et al., 2011; Cook et al., 2011; Herzschuh et al., 2014; Cao et al., 2015). This means that although there might be some mixture of pollen from different sources, the major source should be not far away from the site, i.e. the local area. Secondly, the sedimentary facies are similar among different terraces, implying the major pollen and sediment sources may be comparable.

5.2.2. Vegetation history of the TPRR since the late deglaciation

Unfortunately, the records from the terraces are not continuous; we may only deduce the history from the preserved stages. Fortunately, in this study, the revealed stages are from three critical time intervals: the late deglaciation, mid-Holocene and the late Holocene (Fig. 6G).

5.2.2.1. The late deglaciation (11–14 ka).
A tremendous amount of spores and a variety of broadleaved pollen taxa, such as Anarcadiaceae, *Castanopsis*, Myrtaceae, Caprifoliaceae, Protaceae, Araliacae, Sapindaceae, Oleaceae and Taxodiaceae, represent a tropical/subtropical evergreen forest landscape that quite resembles today's low elevations of Daxue Mountain, lower reaches of Lancang Valley. Some typical components of coniferous and broadleaved mixed forest, like *Pinus*, *Tsuga*, *Quercus*, *Carpinus*, *Ulmus*, *Tilia*, etc. are also common or abundant during this time. It is reasonable to deduce that these types were most likely from the local forests in the valley along the river, when the environments in the valley were much moister than today.

However, we also see a mixing of pollen from multiple vegetation types which are distributed at different elevations today. The assemblage of *Abies*, *Picea*, Ericaceae, *Betula* and Rosaceae etc. is very similar to that observed in the modern pollen rain of alpine forests/shrubs on nearby Baima Mountain; the pollen abundances of *Abies* and *Picea* are even higher than those in modern surface samples of *Abies/Picea* forests. The indicators of alpine meadows, like Polygonaceae, Cyperaceae, Ranunculaceae, Asteraceae, Caryophyllaceae, Scrophulariceae, Onagraceae, Geraniaceae, etc. are all well expressed in the spectra. Hence, the plants forming the modern elevational gradient in vegetation were present in the valley. The *Abies/Picea* forests and the alpine vegetation might have expanded down-slope to a much lower elevation than their present distribution, increasing their representation in the record. The pollen from different vegetation types was probably flushed into the river by the then strengthened surface runoffs (probably due to higher precipitations and/or more melt water from the mountain glacials), leading to a composite vegetation signal of both low and high elevations. Or alternatively, the then vegetation at low elevations integrated components of several vegetation types that are not overlapped today. There were possibly no-analog plant associations in the valley due to the individualistic response of plant taxa to climate change (Williams et al., 2004).

The general pattern is sometimes interrupted by overwhelming local pollen signals in the spectra. The abundant Cyperaceae and Poaceae pollen may suggest well-developed wetlands near the riversides. The broadleaved tree pollen, such as Anarcadiaceae, *Castanopsis*, Caprifoliaceae, Myrtaceae and Rosaceae, which briefly increase to extreme abundances, might also be from locally growing plants. These local plants, together with abundant ferns, also imply a mesic vegetation type, which is distinct from the savanna that dominates the low elevations today.

In summary, the late deglaciation vegetation of the TPRR features a mixed flora that today would be found growing at different elevations with representation from tropical/subtropical evergreen forest to alpine meadow. Whereas the *Abies/Picea* forests dominated the higher part of the valleys, the tropical/subtropical evergreen forests and coniferous and broadleaved mixed forests were probably constrained to limited elevation ranges. Meanwhile, sporadic Amaranthaceae, relatively rare *Artemisia* and absence of drought-tolerant shrubs like Thymelaeaceae do not seem to support the occurrence of valley savannas. This implies much weakened eco-cline from lower to upper reaches of the Lancang valley compared with today.

5.2.2.2. The mid-Holocene (4–7 ka).
Pollen assemblages of this time slice demonstrate a great similarity to those of modern savanna surface samples. Abundant *Artemisia* and Amaranthaceae pollen indicates a drier environment than today, and widespread herbs occupied the landscapes. Meanwhile, the pollen assemblages of Thymelaeaceae, Leguminosae, Anarcadiaceae, Euphorbiaceae and Rubiaceae are also highly comparable with those in the modern savannas. The rarity of Cyperaceae and Poaceae indicate a reduction in wetland habitats in most of the region due to the arid conditions. The environments at low elevations were therefore quite like today, but the savanna habitats were more widespread.

The lack of alpine pollen taxa, such as *Abies*, *Picea*, *Betula*, Ericaceae, Rosaceae, Caryophyllaceae and Geraniaceae, may imply the alpine forests, shrubs and meadows had moved upslope due to a much warmer climate. Quite a small proportion of *Pinus*, *Quercus*, Aceraceae and *Ulmus* pollen relative to contemporary mid-montane surface samples suggests the coniferous and broadleaved mixed forest might also have contracted.

5.2.2.3. The late Holocene (~2 ka).
The climate conditions during this time seem cooler but moister than during the mid-Holocene, but warmer and drier than during the late glacial time. The increased abundances of *Pinus*, *Abies* and *Picea* pollen indicated that the populations of montane conifers were larger than during the mid-Holocene. Moderately abundant Polygonaceae, Asteraceae and Cyperaceae pollen may imply increased alpine meadows. A relatively low abundance of *Artemisia*, Amaranthaceae and Poaceae reflects that
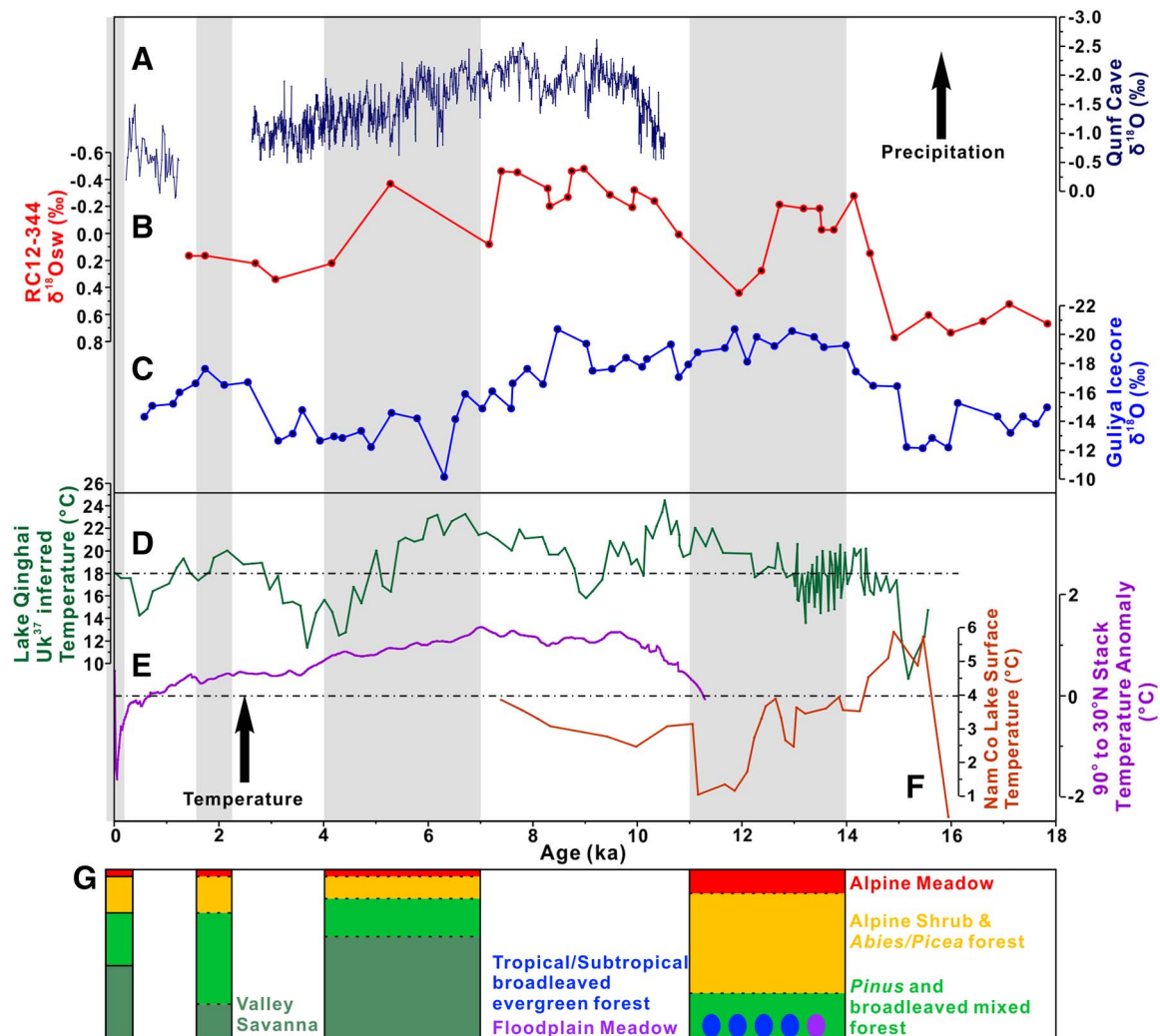
Fig. 6. Comparison of the reconstructed late Quaternary vegetation history in the Three Parallel Rivers region with other palaeoclimate records. Top panel: records of Indian summer monsoon climate. (A) Cave $\delta^{18}O$ record from southern Oman (Fleitmann et al., 2003). (B) $\delta^{18}Osw$ of core RC12-344 from Andaman Sea (Rashid et al., 2007). (C) Ice core $\delta^{18}O$ records from Guliya (Thompson et al., 1997), the timescale is adjusted following Cheng et al., 2011. Middle panel: records of regional palaeotemperature. (D) U_k^{37} inferred temperature record at Lake Qinghai (Hou et al., 2016). (E) Stacked northern hemisphere anomalies relative to present (Marcott et al., 2013). (F) Mean annual lake surface temperature calculated from TEX_{86} record of Nam Co (Günther et al., 2015). Bottom panel: (G) altitudinal distribution of vegetation in the upper Lancang valley during four time intervals (including the present) since the late deglaciation. Note that the schematic diagram is designed to show the general change in relative abundances of different vegetation types rather than to define their exact elevational ranges, because the pollen record is derived from the fluvial sediments at the bottom of the valley so that it probably integrates the vegetation signal along the entire elevational transect.

savanna vegetation existed, but was distributed within a smaller range. The major difference between this time interval and today thus possibly emerges at low elevations. We may consider the vegetation of this late Holocene section to be the relatively natural vegetation before the industrial-era disturbances.

5.2.3. Regional climate changes and impacts on vegetation

The regional climatic conditions could also refer to the non-pollen reconstructions of paleotemperature over the Tibetan Plateau and precipitation in the monsoonal Asia. The TEX_{86} proxy at Lake Nam Co, southern Tibetan Plateau, revealed that the mean air temperature during late deglaciation was ~2 °C colder than present (Fig. 6F) (Günther et al., 2015). Going northward, U_{37}^k index of Lake Qinghai also suggests a cooling of 2–4 °C during 12–14 ka (Fig. 6D) (Hou et al., 2016). Both alkenone records of Lake Qinghai (Hou et al., 2016) and Lake Herleg (Zhao et al., 2013), northern Tibetan Plateau, documented a mid-Holocene thermal maximum that can be compared with the global temperature reconstructions (Marcott et al., 2013). This warmth is followed by a general cooling through the late Holocene (Fig. 6E) (Marcott et al., 2013; Hou et al., 2016).

The stalagmite $\delta^{18}O$ records from Timta cave (Sinha et al., 2005)

and Xiaobailong cave (Cai et al., 2015) all exhibit more negative values during the Bølling-Allerød period (14.7–12.7 ka) than modern monitoring, indicating stronger Indian monsoon and/or enhanced precipitation during the late deglaciation. This finding is generally consistent with the seawater $\delta^{18}O$ record from Andaman Sea that indicates lower salinity and thus stronger Indian monsoon intensity during 14.5–12.6 ka than present (Fig. 6B) (Rashid et al., 2007). Similarly, the δD record from Lake Nam Co was more depleted than present value during 14–7 ka and implies much higher amounts of precipitation then (Günther et al., 2015). Both the Andaman Sea $\delta^{18}O$ record (Rashid et al., 2007) and Qunf stalagmite $\delta^{18}O$ record (Fig. 6A) (Fleitmann et al., 2003) revealed a gradual weakening of summer monsoon to modern levels after the early Holocene maximum (~9.5–7 ka). This broad picture is also supported by various proxies of monsoon precipitation (weathering indicators, magnetic susceptibility and organic $\delta^{13}C$) from Lake Naleng (Opitz et al., 2015).

The Guliya ice core $\delta^{18}O$ record (Fig. 6C) provides another important reference to late Quaternary climate changes over the Tibetan Plateau (Thompson et al., 1997). Traditionally, it has been used as a benchmark for regional temperature, and accordingly, the late deglaciation (15–11 ka) was similar to or even warmer than present

([Thompson et al., 1997](#)). However, its age model has recently been questioned for the lack of robust absolute datings. [Cheng et al. (2012)](#) found that precipitation documented by the stalagmite $\delta^{18}O$ record from Kesang cave changed inversely to that documented by Guliya ice core, although both sites share a common moisture source today. To reconcile this difference, they proposed a revision in the Guliya chronology by negatively, rather than positively, matching the Guliya $\delta^{18}O$ record with the GISP2 CH_4 record. This results in a shrinking of the Guliya time scale by a factor of two, but similar isotopic variations at both sites. After such a revision, the late deglaciation ice core $\delta^{18}O$ values were most depleted instead of enriched, and possibly indicate heavy precipitation instead of high temperatures. Here we will take the latter interpretation as it is coherent with other lines of evidences mentioned above.

Our results from the vegetation reconstruction ([Fig. 6](#)G) are consistent with the regional pattern. In the TPRR, it was cold and wet during late deglaciation, warm and dry in the mid-Holocene, and cool and dry in the late Holocene. Apparently, the environments were affected or controlled by some regional factors. A good candidate is the variation of the Indian summer monsoon. The late deglacial expansion of alpine forest corresponds to the decreased temperature. Meanwhile, the tropical/subtropical forest retained at low elevations under stronger Indian summer monsoon and more precipitation. As the Indian summer monsoon was weakened during mid-to-late Holocene, the tropical/subtropical forests were extirpated from the TPRR, and gave way to valley savanna. The mid-Holocene warmth compressed the distribution of the alpine vegetation on one hand, and on the other it might have accelerated the evaporation, intensified the drought and thus promoted the expansion of savanna at low elevations.

Concerning the biodiversity, the frequent shifts in plant elevation ranges associated with regional warming or cooling are verified. Considering the complexity of the geomorphology, plant communities might have isolated frequently on the peaks or in the valleys to form some microrefugia for some ecosystems ([Rull, 2009; Mosblech et al., 2011](#)). Biotic mixing and possibly related sympatric speciation, hybridization and polyploidy therefore could be expected along the slopes ([Rull, 2005; Mosblech et al., 2011](#)). Moreover, the longitudinal migration of plant taxa, which was probably linked with monsoon variability and might promote the communication with Southeast Asian elements, was previously neglected in the diversification model. Interestingly, the alpine and mid-montane vegetation, which holds the major species richness in this region ([Zhang et al., 2009](#)), was more fragmented during the mid-Holocene than the glacial period due to the combined effect of warmth and drought. This indicates that the plant communities of the TPRR are more likely to be stressed by heat in the interglacial period. Consequently, the time when we think of these species needing to exist in refugia is during the interglacial rather than the glacial. The climate-induced vicariance ([Rull, 2005](#)) thus might have centered on past interglacials given that the ice ages compose the majority of Quaternary history. In a CO_2-induced warming future, most species are expected to meet their population bottlenecks in this mountainous region. Following the "wet wetter, dry drier" principle ([Held and Soden, 2006](#)), the low elevation savanna might expand, further insulate the alpine vegetation, and increase the difficulty of conservation.

6. Conclusions

Based on the surface samples, the relationship between the modern pollen rain and contemporary vegetation of the TPRR is clarified. The valley savanna between 1900 and 3500 m is distinguished by pollen assemblages of *Artemisia*, Amaranthaceae, Poaceae, *Juglans*, Thymelaeaceae, Euphorbiaceae, etc. For *Abies* forests between 3800 and 4100 m, *Abies*, *Picea*, *Quercus*, *Betula*, Rosaceae are characteristic, and for alpine shrub between 4000 and 4350 m, Ericaceae, Ranunculaceae are the best indicators. Alpine meadows between 4350

and 4500 m are recognized by abundant Polygonaceae and Cyperaceae. The contemporary vegetation is thus generally well reflected in the pollen spectrum except for the ambiguous *Pinus* and broadleaved mixed forest between 3000 and 3800 m.

By extrapolating these modern correlations, fossil pollen records from late-Quaternary fluvial terrace sediments along the Lancang valley are interpreted to mainly document the changes in elevation range of the regional vegetation, with limited local (i.e. vegetation on the floodplain, point bar, etc.) and upstream (i.e. vegetation over the Tibetan Plateau) signals. Accordingly, the *Abies/Picea* forests covered a larger area than currently present during the late deglaciation due to the temperature drop. Subtropical/tropical broadleaved evergreen forests, which today commonly occur to the south (lower stream of the river), occupied the low elevation landscapes under a wetter climate. But these forests have retreated from the valleys since the mid-Holocene, probably in response to the weakening of Indian summer monsoon. The montane forests may have experienced the most extensive contraction during the period of mid-Holocene warmth, and re-expanded to current distribution. In general, the vegetation history of the TPRR through several time windows of past 14 ka clearly demonstrates a sensitivity of altitudinal distribution of vegetation to past climate changes. While temperature provides the major control in the montane vegetations (broadleaved and coniferous mixed forest, *Abies* forest, alpine shrub and alpine meadow), the base vegetations (savanna or broadleaved evergreen forest) are more prone to be influenced by precipitation.

References

Bonny, A.P., 1978. The effect of pollen recruitment processes on pollen distribution over the sediment surface of a small lake in Cumbria. J. Ecol. 66, 385–416.

Brown, A.G., 1985. The potential use of pollen in the identification of suspended sediment sources. Earth Surf. Process. Landf. 10, 27–32.

Brown, A.G., Carpenter, R.G., Walling, D.E., 2008. Monitoring the fluvial palynomorph load in a lowland temperate catchment and its relationship to suspended sediment and discharge. Hydrobiologia 607, 27–40.

Cai, Y.J., Fung, I.Y., Edwards, R.L., An, Z.S., Cheng, H., Lee, J.E., ... Chiang, J.C.H., 2015. Variability of stalagmite-inferred Indian monsoon precipitation over the past 252,000 y. Proc. Natl. Acad. Sci. 112, 2954–2959.

Cao, X.Y., Herzschuh, U., Ni, J., Zhao, Y., Böhmer, T., 2015. Spatial and temporal distributions of major tree taxa in eastern continental Asia during the last 22,000 years. The Holocene 25, 79–91.

Cheng, H., Zhang, P.Z., Spötl, C., Edwards, R.L., Cai, Y.J., Zhang, D.Z., ... An, Z.S., 2012. The climatic cyclicity in semiarid-arid central Asia over the past 500,000 years. Geophys. Res. Lett. 39, 1705–1709.

Chmura, G.L., Liu, K.B., 1990. Pollen in the lower Mississippi River. Rev. Palaeobot. Palynol. 64, 253–261.

Chmura, G.L., Smirnov, A., Campbell, I.D., 1999. Pollen transport through distributaries and depositional patterns in coastal waters. Palaeogeogr. Palaeoclimatol. Palaeoecol. 149, 257–270.

Cook, C.G., Jones, R.T., Langdon, P.G., Leng, M.J., Zhang, E.L., 2011. New insights on late Quaternary Asian palaeomonsoon variability and the timing of the Last Glacial Maximum in southwestern China. Quat. Sci. Rev. 30, 808–820.

Cun, Y.Z., Wang, X.Q., 2010. Plant recolonization in the Himalaya from the southeastern Qinghai-Tibetan Plateau: geographical isolation contributed to high population differentiation. Mol. Phylogenet. Evol. 56, 972–982.

Dutta, S., Suresh, N., Kumar, R., 2012. Climatically controlled Late Quaternary terrace staircase development in the foldand-thrust belt of the Sub Himalaya. Palaeogeogr. Palaeoclimatol. Palaeoecol. 356, 16–26.

Fall, P.L., 1987. Pollen taphonomy in a canyon stream. Quat. Res. 28, 393–406.

Fleitmann, D., Burns, S.J., Mudelsee, M., Neff, U., Kramers, J., Mangini, A., Matter, A., 2003. Holocene forcing of the Indian monsoon recorded in a stalagmite from southern Oman. Science 300, 1737–1739.

Fujiki, T., Zhou, Z.K., Yasuda, Y., 2005. The Pollen Flora of Yunnan China. Roli Books, New Delhi.

Günther, F., Witt, R., Schouten, S., Mäusbacher, R., Daut, G., Zhu, L.P., ... Gleixner, G.,

2015. Quaternary ecological responses and impacts of the Indian Ocean Summer Monsoon at Nam Co, Southern Tibetan Plateau. Quat. Sci. Rev. 112, 66–77.

Guo, L.Q., 2004. Geological dividing of forests at Three Parallel Rivers of Yunnan protected areas. J. West Chin. For. Sci. 33, 10–16.

Hall, S.A., 1989. Pollen analysis and paleoecology of alluvium. Quat. Res. 31, 435–438.

Held, I.M., Soden, B.J., 2006. Robust response of the hydrological cycle to global warming. J. Clim. 19, 5686–5699.

Herzschuh, U., Borkowski, J., Schewe, J., Mischke, S., Tian, F., 2014. Moisture-advection feedback supports strong early-to-mid Holocene monsoon climate on the eastern Tibetan Plateau as inferred from a pollen-based reconstruction. Palaeogeogr. Palaeoclimatol. Palaeoecol. 402, 44–54.

Holmes, P., 1990. Differential transport of spores and pollen—a laboratory study. Rev. Palaeobot. Palynol. 64, 289–296.

Holmes, P., 1994. The sorting of spores and pollen by water: experimental and field evidence. In: Sedimentation of Organic Particles. Cambridge University Press, Cambridge, pp. 9–32.

Hou, J.Z., Huang, Y.S., Zhao, J.T., Liu, Z.H., Colman, S., An, Z.S., 2016. Large Holocene summer temperature oscillations and impact on the peopling of northeastern Tibetan Plateau. Geophys. Res. Lett. 43, 1323–1330.

Jarvis, D.I., Leopold, E.B., Liu, Y.Q., 1992. Distinguishing the pollen of deciduous oaks, evergreen oaks and certain rosaceous species of southwestern Sichuan Province, China. Rev. Palaeobot. Palynol. 75, 259–271.

Ji, F.J., Zheng, R.Z., Li, J.P., Yin, J.H., 2000. Chronological research of geomorphic surface of lower terraces along several major rivers in the east and west of Yunnan Province. Seismol. Geol. 22, 265–276.

Kramer, A., Herzschuh, U., Mischke, S., Zhang, C.J., 2010. Late glacial vegetation and climate oscillations on the southeastern Tibetan Plateau inferred from the Lake Naleng pollen profile. Quat. Res. 73, 324–335.

Li, N., 1995. Studies on the geographic distribution, origin and dispersal of the family Pinaceae Lindl. Acta Phytotaxon. Sin. 33, 105–130.

Li, X.W., Li, J., 1993. A preliminary floristic study on the seed plants from the region of HengDuan Mountain. Acta Bot. Yunnanica 15, 217–231.

Li, W.H., Zhang, Y.G., 2010. Vertical Climate in HengDuan Mountains and Its Influence on the Distribution of Forest. China Meteorological Press, Beijing.

Li, Q., Lu, H.Y., Zhu, L.P., Wu, N.Q., Wang, J.B., Lu, X.M., 2011. Pollen-inferred climate changes and vertical shifts of alpine vegetation belts on the northern slope of the Nyainqentanglha Mountains (central Tibetan Plateau) since 8.4 kyr BP. The Holocene 21, 939–950.

Ma, H.C., Jack, A.M., 2001. The dry-hot valleys and forestation in southwest china. J. For. Res. 12, 35–39.

Marcott, S.A., Shakun, J.D., Clark, P.U., Mix, A.C., 2013. A reconstruction of regional and global temperature for the past 11,300 years. Science 339, 1198–1201.

Mosblech, N.A.S., Bush, M.B., van Woesik, R., 2011. On metapopulations and microrefugia: palaeoecological insights. J. Biogeogr. 38, 419–429.

Myers, N., Mittermeier, R.A., Mittermeier, C.G., da Fonseca, G.A., Kent, J., 2000. Biodiversity hotspots for conservation priorities. Nature 403, 853–858.

Nie, Z.L., Wen, J., Gu, Z.J., 2005. Polyploidy in the flora of the Hengduan Mountains hotspot, Southwestern China. Ann. Mo. Bot. Gard. 92, 275–306.

Opitz, S., Zhang, C.J., Herzschuh, U., Mischke, S., 2015. Climate variability on the southeastern Tibetan Plateau since the Lateglacial based on a multiproxy approach from Lake Naleng—comparing pollen and non-pollen signals. Quat. Sci. Rev. 115, 112–122.

Pan, T., Wu, S.H., Dai, E.F., Liu, Y.J., Dou, Y., 2009. Significance of pollen and spores distribution to the barrier function of the longitudinal range-gorge region, Southwest China. J. Geogr. Sci. 19, 660–670.

Peck, R.M., 1973. Pollen budget studies in a small Yorkshire catchment. In: Quaternary Plant Ecology. Blackwell Scientific Publications, Oxford, pp. 43–60.

Rashid, H., Flower, B.P., Poore, R.Z., Quinn, T.M., 2007. A 25 ka Indian Ocean monsoon variability record from the Andaman Sea. Quat. Sci. Rev. 26, 2586–2597.

Rull, V., 2005. Biotic diversification in the Guayana Highlands: a proposal. J. Biogeogr. 32, 921–927.

Rull, V., 2009. Microrefugia. J. Biogeogr. 36, 481–484.

Schweinfurth, U., 1975. Exploration in the Eastern of the Himalayas and the river gorge country & southeastern Tibet-Francis Kingdom Ward. Geogr. Res. 3, 1–102.

Shen, J., Liu, X.Q., Wang, S.M., Ryo, M., 2005. Palaeoclimatic changes in the Qinghai Lake area during the last 18,000 years. Quat. Int. 136, 131–140.

Shen, C.M., Liu, K., Tang, L.Y., Overpeck, J.T., 2006. Quantitative relationships between modern pollen rain and climate in the Tibetan Plateau. Rev. Palaeobot. Palynol. 140, 61–77.

Simirnov, A., Chmura, G.L., Lapointe, M.F., 1996. Spatial distribution of suspended pollen in the Mississippi River as an example of pollen transport in alluvial channels. Rev. Palaeobot. Palynol. 92, 69–81.

Sinha, A., Cannariato, K.G., Stott, L.D., Li, H.C., You, C.F., Cheng, H., ... Singh, I.B., 2005. Variability of Southwest Indian summer monsoon precipitation during the Bølling/Allerød. Geology 33, 813–816.

Thompson, L.G., Yao, T.D., Davis, M.E., Henderson, K.A., Mosley-Thompson, E., Lin, P., Bolzan, J.F., 1997. Tropical climate instability: the last glacial cycle from a Qinghai-Tibetan ice core. Science 276, 1821–1826.

United Nations Educational Scientific and Cultural Organization (UNSCO), 2003. Three Parallel Rivers of Yunnan protected areas. http://whc.unesco.org/en/list/1083.

Wang, F.X., Chinen, N.F., Zhang, Y.L., Yang, H.Q., 1991. Pollen Flore of China. Science Press, Beijing.

Wang, A., Smith, J.A., Wang, G.C., Zhang, K.X., Xiang, S.Y., Liu, D.M., 2009. Late Quaternary river terrace sequences in the eastern Kunlun Range, northern Tibet: a combined record of climatic change and surface uplift. J. Asian Earth Sci. 34, 532–543.

Wei, H.C., Ma, H.Z., Zheng, Z., Pan, A.D., Huang, K.Y., 2011. Modern pollen assemblages of surface samples and their relationships to vegetation and climate in the northeastern Qinghai-Tibetan plateau. Rev. Palaeobot. Palynol. 163, 237–246.

Williams, J.W., Shuman, B.N., Webb III, T., Bartlein, P.J., Leduc, P.L., 2004. Late-Quaternary vegetation dynamics in North America: scaling from taxa to biomes. Ecol. Monogr. 74 (2), 309–334.

Wischnewski, J., Mischke, S., Wang, Y.B., Herzschuh, U., 2011. Reconstructing climate variability on the northeastern Tibetan Plateau since the last Lateglacial—a multiproxy, dual-site approach comparing terrestrial and aquatic signals. Quat. Sci. Rev. 30, 82–97.

Wu, Z.Y., 1988. Hengduan Mountain flora and her significance. J. Jpn. Bot. 58, 49–56.

Xiao, X.Y., Tong, S.M., Shen, J., Wang, S.M., Yang, X.D., Tong, G.B., 2009. Altitudinal distribution of surface pollen and their relations to modern vegetation in the Yulong mountains, Yunnan Province. Quat. Sci. 29, 80–88.

Xiao, X.Y., Haberle, S.G., Shen, J., Yang, X.D., Han, Y., Zhang, E.L., Wang, S.M., 2014. Latest Pleistocene and Holocene vegetation and climate history inferred from an alpine lacustrine record, northwestern Yunnan Province, southwestern China. Quat. Sci. Rev. 86, 35–48.

Xu, Q.H., Yang, X.L., Wu, C., Meng, L.Y., Wang, Z.H., 1996. Alluvial pollen on the North China Plain. Quat. Res. 46, 270–280.

Yu, G., Tang, L.Y., Yang, X.D., Ke, X.K., Harrison, S.P., 2001. Modern pollen samples from alpine vegetation on the Tibetan Plateau. Glob. Ecol. Biogeogr. 10, 503–519.

Zhang, R.Z., Zheng, D., Yang, Q.Y., Liu, Y.H., 1997. Physical Geography of Hengduan Mountains. Science Press, Beijing.

Zhang, D.C., Zhang, Y.H., Boufford, D.E., Sun, H., 2009. Elevational patterns of species richness and endemism for some important taxa in the Hengduan Mountains, southwestern China. Biodivers. Conserv. 18, 699–716.

Zhao, Y., Herzschuh, U., 2009. Modern pollen representation of source vegetation in the Qaidam Basin and surrounding mountains, north-eastern Tibetan Plateau. Veg. Hist. Archaeobotany 18, 245–260.

Zhao, Y., Yu, Z.C., Zhao, W.W., 2011. Holocene vegetation and climate histories in the eastern Tibetan Plateau: controls by insolation-driven temperature or monsoon-derived precipitation changes? Quat. Sci. Rev. 30, 1173–1184.

Zhao, C., Liu, Z.H., Rohling, E.J., Yu, Z.C., Liu, W.G., He, Y.X., ... Chen, F.H., 2013. Holocene temperature fluctuations in the northern Tibetan Plateau. Quat. Res. 80, 55–65.

Zhu, Y., Chen, F.H., Cheng, B., Zhang, J.W., Madsen, D.B., 2002. Pollen assemblage features of modern water samples from the Shiyang River drainage, arid region of China. Acta Bot. Sin. 44, 367–372.

Zhu, Y., Xie, Y.W., Cheng, B., Chen, F.H., Zhang, J.W., 2003. Pollen transport in the Shiyang River drainage, arid China. Chin. Sci. Bull. 48, 1499–1506.